SURFACE STUDIES AND ELECTRON EMISSIONS

A. SEPTIER, CNAM, 292 rue Saint-Martin, 75141 Paris Cedex 03
and IEF, Université Paris-Sud, 91405 Orsay (France).

INTRODUCTION

One of the aims of modern surface analysis is to determine the physical and chemical structure of the surface layer of the sample. The physical structure includes topography and morphology of the surfaces on a micron and submicron scale , and the arrangement of atoms in a lattice as well as the extent, shape and type of lattice defects. The chemical structure is the distribution and concentration of elements in a surface layer on a micron or submicron scale. It can be determined with various beam techniques such as Auger spectroscopy (AES), X-ray photoelectron spectroscopy (XPS), ion scattering spectroscopy (ISS), secondary ion mass spectroscopy (SIMS), electron probe microanalysis (EPM).

Size and shape of crystals or grain boundaries, chemical composition of small inclusions, and size and type of lattice defects can be studied by electron microscopy and electron diffraction.

All methods have their advantage and disadvantage, and must be considered as complementary techniques. The optimum choice of the methods to be used depends on the problem being investigated [1].

In all analysing methods, information about the atoms or molecules contained in the surface layer, are given by particles - ions or electrons - emitted by the sample, which can be bombarded by photons, electrons or ions. But in the most commonly used methods, the information depth, which corresponds to the escape length of the outgoing particles, is often limited to a few angströms, and to perform a chemical analysis of a layer in the micron range it is therefore necessary to remove progressively the sample surface, by ion sputtering. A depth profile of one particular element can be obtained by sequential sputtering and analysis, using either AES, UPS or XPS . A continuous analysis during sputtering is also possible by a SIMS technique.

All these methods are destructive, and a scrutiny of the results is necessary, as the ion bombardment may introduce many artefacts and often has a non negligible influence on the resolution and on in-depth profiling.

Several other methods are able to provide depth profiling of one element without destroying the surface layer: Rutherford backscattering spectrometry and Nuclear microanalysis. In the first method He^+ ions are used, and for a fixed angle of observation, the energy of backscattered ions is at the same time a known function of the nature of the atom hitted by the incident ion, and of the distance from the surface where the collision takes place. The energy spectrum of the backscattered ion may be directly converted into a in-depth repartition of the analyzed element.

Nuclear microanalysis is possible only with a few number of elements [2] which are able to give radioactive nuclei, when bombarded by D^+ or H^+ ions. For example, oxygen O^{16} and nitrogen N^{14} atoms bombarded by 2 MeV deuterons give O^{17} and C^{12}, after emission of a proton or an α particle, respectively.

The number of secondary protons or α particles is proportional to the oxygen - or nitrogen - content, and energy analysis of these particles give the depth profile of the impurities in the lattice.

As far as very thin surface layers are concerned, in the 50 - 200 Å range, X-ray photon spectroscopy (XPS) may be used, combined with an angular energy analysis of the emitted Auger electrons, to obtain the thickness of contaminated or oxidized layers, grown on the surface of the sample.

After this short review of the most familiar surface analysis techniques, which all have to be performed in an UHV chamber in order to avoid additional contamination of the surface, I shall briefly report on works concerning superconducting material surfaces, essentially niobium or niobium-tin.

In the first part, I will talk essentially about chemical properties of the Nb surfaces, and surface studies.

The second part will be devoted to another very important aspect of surface properties: electron emission from clean or contaminated surfaces.

PART I. SURFACE STUDIES

1. THIN FILMS

1.1 - Nb

The RF performances of sputtering thin films of Nb may be lessened by several defects: lack of uniform coverage, strains, Ar ion in the neutral lattice, gettering of contaminants by the freshly deposited material. An approach has been made [3] to evaluate the potentiality of sputtering technique by measuring RF properties of sputtered Nb coating, and using Nb as the substrate material in order to minimize the mismatch between expansion coefficients of substrate and coating. A Q_o of 3×10^9 and a peak magnetic field of 205 Gauss were achieved, demonstrating that the sputtering technique is capable of producing Nb surfaces of good quality, at the condition that the shape of the cavity be simple enough to obtain an uniform film thickness.

In contrast, and certainly due to the strains between the substrate and the Nb films, surface resistances of Nb films sputtered on a Cu substrate, were 100 times greater than for bulk Nb .

1.2 - Nb_3Sn

Nb_3Sn is generally used in thick layers grown on Nb surfaces. A second way to use Nb_3Sn is as a covering for the Nb surface that is a few monolayers thick [4]. It would be hoped that the Nb_3Sn would not be as sensitive to O_2 as pure Nb, and would form a high-T_c protective surface without introducing normal excitation. Since the layer would be much thinner that the coherence length, the losses would be determined mainly by the surface resistance of the Nb underneath.

The better quality films with a sharp transition and critical temperatures of about 16 K were produced by alternatively depositing layers of Sn and then annealing temperature ranging from 800 to 900 °C . Critical tempera-

tures are lowered by the proximity effect, varying from about 9 K for à Nb_3Sn thickness of 100 Å to about 15 K for a layer of 1000 Å thick. Nb_3Sn thin films with high T_c appear fairly uniform, with a large grain size. Other films which show a broad transition also show a rougher surface, as observed by optical and scanning electron microscopy.

After an exposure to the air, the films were measured again. Relatively small shifts in the transition curves of Nb_3Sn were observed, proving that even the thin Nb_3Sn is relatively stable in air.

1.3 - The influence of crystal orientation on the quality of Nb_3Sn layers has been studied in several laboratories and more recently by the Siemens group (5), using observation with light and scanning electron microscope, and chemical analysis by AES. The Nb_3Sn layers were grown on Nb substrates oriented along the (100) (110) (111) and (531) directions respectively. For each orientation, one substrate was chemically polished (CP), and another one CP and then oxipolished. On the CP substrates, the Nb_3Sn layer was discontinuous, and the holes may corresponds to 50 % of the total area for the (111) orientation. On the contrary, there is no difference in the structure of the continuous Nb_3Sn structure growing on the oxipolished substrates. It seems that oxipolishing makes easier the nucleation of Nb_3Sn on the surface and then allows an homogeneous growing of a dense Nb Sn layer, whatever may the orientation of the Nb lattice.

Auger analysis show that the ratio between Sn and Nb signals is higher for oxipolished samples; without differences due to the orientation of the substrate, and that the Nb_3Sn layer may be considered as fairly homogeneous. On the contrary, the Nb_3Sn layer grown on substrates only chemically polished, is poor in Sn, except on the outer layers where a correct stoechiometric composition is obtained.

Oxipolishing seems a necessary procedure to obtain Nb_3Sn layers of a good quality, in addition to an clean preparation technique.

II. SURFACE IMPURITIES

2.1 - Carbon

Surface of reactor grade electron beam melted Nb have been examined (6) using a scanning electron microscope, equipped with a crystal X-ray spectrometer. The presence of carbon inclusions has been established, occuring primarily at grain boundaries. In an unfired chemically polished sample, 50 carbonaceous inclusions per cm^2 were observed, with an average diameter of 10 µm, corresponding to a volume concentration of C of approximatively 16 ppm . Another sample, which was fired for 7 hours at 2100 °C, at 10^{-8} Torr, was also examined. The number of carbonaceous inclusions was lowered by a factor of 4, and the total carbon concentration by a factor of 6, compared to the chemically polished sample.

The presence of carbon on a fired Nb cavity surface has been also observed in electron microprobe studies at SLAC (7). The carbon tends to occur as inclusions with dimensions on the order of 10 microns, frequently located at crystal boundaries. They can presumably become regions of enhanced local heating leading to magnetic breakdown.

Several techniques have been successfully used to remove the carbon:

- anodization of the cavity before the final firing,
- or heating the cavity at 1900 °C during one hour in an oxygen atmosphere at pressure of 7×10^{-6} Torr .

The role of oxygen is further clarified by observations made using a residual gas analyzer during HT treatment in oxygen; an heavy evolution of CO_2 and CO is seen during the initial stage of firing.

On Auger spectra a strong carbon signal is generally observed. This carbon signal is weakest for an anodized surface, intermediate for a furnace cleaned surfaces and strongest after chemical treatments (8). Decarburization by means of a furnace treatment of an anodized surface gives a low carbon signal.

Carbon present on Nb surfaces may have different origins: (i) carbon diffusing to the surface from the volume of the sample, the C natural concentration in the best quality Nb being of the order of 15 - 20 ppm ; (ii) carbon in adsorbed organic molecules, like hydrocarbons, which are residue from cleaning with methanol or aceton ; (iii) carbon in adsorbed CO or CO_2 molecules.

2.2 - Fluorine

Fluorine has been observed by Auger electron spectroscopy on surfaces (8) chemically polished in baths containing HF, or after dissolution of Nb_2O_5 by HF (oxipolishing). F remains detectable within a depth of about 50 Å .

Nuclear analysis has been used to study the contamination by fluorine of samples subjected to various treatments in baths containing fluorhydric acid, for example oxipolishing (9). The reaction F^{19} (p,α) O^{16} is used, when the metal is bombarded with 2 MeV protons. Experiments were carried out with Ta, a metal having chemical properties very similar to those of Nb .

Typically, the metal surface is covered with a 20 - 45 Å of natural oxide and 2×10^{15} at/cm^2 of fluorine are found in films containing 2×10^{16} at/cm^2 of oxygen. Rinsing the sample in boiling water decreases the amount of fluorine by 50 % and the dissolution of the surface contaminated oxide in a NH_4F - FH solution reduces the fluorine contamination to less than 1.5×10^{14} at/cm^2 . After anodic oxidation of the cleaned surface, it was found that after oxide growth the fluorine remains near the metal-oxide interface.

2.3 - Contamination of the oxide

The influence of the nature of the electrolyte on the film formation oxygen yield during anodic oxidation of Nb has been studied by the ENS group in Paris (10).This yield is defined as the ratio of the oxygen contained in the film to the amount of bivalent oxygen equivalent to the oxidation charge.

It has been shown that this ratio is greater than 1 for films formed in concentrated acids, implying a large incorporation of anions characteristic of the acids. The total amount of oxygen may be measured with a good precision by nuclear microanalysis. The samples were bombarded with 2 MeV D^+ ions O^{17} is formed by the reaction O^{16} (d,p) O^{17}, and the concentration of the radioactive element O^{17} is then measured with semiconductor detectors placed near the sample.

From these measurements, the concentration of O^{16} is obtained, by comparison with O^{16} standards with an accuracy estimated as 2 or 3%. The nitrogen concentration may be also measured by using the reaction $N^{14}(d,\alpha)C^{12}$, and counting the emitted α particles.

The oxygen yield R may attain 1.27 when the anodization is carried out in HNO_3, 95% and 1.49 in HCOOH 98%. R increases with acid concentration and tends toward unity at low concentration. The supplementary oxygen atoms are due to anions incorporated in the oxide, NO_3^- for example. Nuclear microanalysis of N^{14} allow a direct determination of nitrogen, in Nb_2O_5 obtained by oxidation in concentrated HNO_3. The quantitative estimation of the anion incorporation rate is deduced from the direct analysis of N. Incorporation of 1 at of N for every 100 at of oxygen has been measured. This corresponds to an incorporation of about 10×10^{14} at/cm^2. Concerning weak electrolytes, it seems that there is a negligible incorporation of nitrogen into the oxide.

In contradiction with these results, Nb_2O_5 grown in NH_3 aqueous solutions may be strongly contaminated by nitrogen, as shown recently [19] by an XPS study.

2.4 - Other contaminants

Sulphur, chlorine are often present on chemically polished surfaces, coming from the acid baths. This contaminants may be eliminated by heat treatment. The titanium pump in an UHV furnace is at the origin of a weak Ti signals in AES spectra [8], and Ti atoms may diffuse to a depth of about 50 Å.

III. ADSORBED GASES. OUTGASSING.

3.1 - Adsorbed gases

The influence of solute oxygen and nitrogen on the magnetic breakdown and residual losses of SC Nb cavities, was investigated experimentally by exposing the cavities to these gases at pressures up to 10^{-5} Torr during the heat treatment at 2100 K [11].

Oxygen may decrease the critical temperature (0.93 K per at %) and the electronic mean free path at the surface, causing low thermal conductivity and a lower critical field H_{c_1}. Layer of NbO - or NbO_2 - are also suggested as surface contaminant. The effects of O_2 are augmented by an enhanced solute concentration at the surface during the cooldown after the normal UHV bakeout. To achieve a desired clean surface it is therefore necessary to reduce the bulk concentration of O_2 to about 1×10^{-3} at %, requiring a partial pressure of 10^{-9} Torr at 2100 K.

A direct measurement of the resistance ratio in the cavity walls by the eddy-current method was performed after a 20 h oxygen exposure. The resistance ratio R remained essentially unchanged at the value of R = 41 implying a mean free path of about 1000 Å in the bulk of the material. No change in the critical temperature, the measured gap and the BCS part in the surface losses due to the gas exposure can be observed.

Solute nitrogen in concentrations up to about 8×10^{-2} at % (125 ppm) has no effect on the peak magnetic field. As to the influence of oxygen, bulk concentrations up to 7.5×10^{-3} at % (13 ppm) do not affect the breakdown field, whereas higher concentrations, above 1.2×10^{-1} at % (200 ppm) cause a definite

reduction in the peak field. The residual Q was in all cases lowered by the oxygen exposure, but the effect is not proportional to the O_2 concentration.

Measurements of the penetration depth $\delta(0)$ of Nb wires, before and after oxygen exposure respectively gives values of $\delta(0) \# 400$ Å and $\delta(0) \simeq 720$ Å respectively. To explain the large penetration depth, it is necessary to assume a mean free path of about 125 Å in the surface sheath - which is an order of magnitude smaller than in the bulk of the material, denoting a substantial oxygen enrichment at the surface. An equally large penetration depth was measured after N_2 exposure. As large penetration depths are associated to low values of the critical field H_{c_1}, we may assume that oxygen is partly responsible for the lowering of the peak field in the cavities containing solute oxygen in their walls.

The effect of various common gases on the RF properties have also been explored at SLAC [12]: the cavities being filled with the gas for about 1 hour. These effects can be profound, particularily with CO_2 and CO which lower the peak magnetic field by a large factor. Dry oxygen, nitrogen, or hydrogen have only a weak influence on the values of the surface resistance and the peak magnetic field.

3.2 - Heat treatment

Four processes take place during HT firing in UHV:

- evaporation of oxides from the surface, in particular metallic NbO, and of volatiles impurities,
- lowering the overall oxygen concentration, and of the carbon concentration,
- thermal polishing,
- enhanced grain growth.

Concerning the removal of oxygen from Nb, LEED can yield the structure of the surface layers of the metal. Because the energy range of the electrons (from about 10 to 500 eV) the electrons penetrate into the sample a few monolayers, and so the diffraction patterns that are obtained are characteristic of these surface layers. The sample initially put in the chamber is heated in UHV at a given temperature T_a and then cooled down quickly in order to obtain the LEED diagram with a good resolution.

The figure 1 shows how difficult it is to remove the last traces of oxygen [4][13]. The intensity of the O_2 line in Auger spectrum is plotted as a function of the sample thermal history, and LEED patterns were taken at room temperature after cooling. In (a), the Nb single-crystal surface is covered with adsorbed oxygen. In (b), after annealing at $T_a = 1000$ °C, a faceted surface is observed, corresponding to a thin layer of a Nb oxide of unknown composition. In (c), for $T_a > 1800$ °C, the oxide layer surface - probably NbO - is again parallel to the substrate. Finally, a clean Nb surface appears for $T_a \geqslant 2000$ °C. (see (d)).

Other experiments show that even at 3×10^{-8} Torr of oxygen at 950 °C oxide structures are formed. Hence a cavity cooling from its heat treatment temperature of 1900 °C will pick-up oxides either from the bulk, or from residual gas in the chamber.

AES was used [14] to study the amount of gases that diffuse to the surface as the sample is cooled. In a partial oxygen pressure of 3×10^{-8} Torr,

a sample was heated to about 1400 °C during 9 minutes. While hot, the Auger pattern shows that the O concentration on the surface is less than 1/10 of a monolayer.

Upon cooling, Auger spectra are recorded and the spectrum obtained 45 sec after the beginning of the cooling process show that almost a monolayer of O is detectable, indicating a diffusion from the bulk. In effect, at the ambient pressure of 3×10^{-9} Torr, there is not enough gas hitting the sample to account for the rapid build-up of oxygen on the surface.

Since RF fields react with the metal in a very thin layer of $\sim$ 500 Å only, the surface preparation is extremely important to achieve high Q and high surface fields. Oxygen contaminated layers would have a lower T_c and poorer microwave performances. A layer of the semimetal NbO would also affect adversely the microwave properties.

It would be of great value to have a stable surface condition, for ease in handling the RF cavities. Several possibilities have been proposed for protecting the Nb surfaces: (i) anodic oxidation, due to the conversion of various oxide into Nb_2O_5, that is a low-loss insulator; (ii) covering the surface with a thin layer of some high-T_c material as Nb_3Sn or NbN .

It is not yet clear what surface properties are the most important for achieving high Q and high peak RF fields. The answer to this question will be provided by a careful correlation between microwave cavity measurements and surface studies on small samples processed at the same time. It is possible than suitable surface coatings may finally provide the best solution.

IV. OXIDATION OF Nb AND Nb_3Sn

Several methods have been used to study the oxidation of clean Nb surfaces, to determine exact composition, structure and thickness of the various oxides always present on real Nb surfaces exposed to air or even to very low residual gas pressures in a UHV chamber.

4.1 - Ellipsometry

Ellipsometry, have been used to study Nb oxide growing on a Nb surface by plasma oxidation [15]. It was possible to test various treatments of the surface to find the one that give the cleanest surface possible prior to growth of the plasma oxide. The best treatment was found to consist of heating the sample at HT in high vacuum. Ar and O_2 were admitted both to a partial pressure of 0.05 Torr, and a glow discharge was turned on. About 6 hours were necessary to grow 1500 Å of oxide. From the ellipsometric data it was possible to calculate the refractive index $n = 2.30 + i\ 0$ for Nb oxides, and $n' = 3.0 + i\ 3.6$ for the Nb substrate. We shall emphasize the confirmation that - at least for optical frequencies - Nb_2O_5 is a perfect dielectric material.

To improve the properties of tunnel Josephson junctions. In situ ellipsometric measurements have been made at IBM during growth of the tunnel oxide on the base electrode in a RF plasma [16] , and the results were compared with electrical measurements. Two additional processes are found to have an important influence on the junction characteristics: precleaning of the base electrode in an argon plasma before oxidation, and a further treatment of the grown

oxide in a low voltage discharge in order to remove the adsorbed residual gases. The most effective gas for this process is nitrogen. The oxides were fabricated in a controlled RF process using Ar/O_2 mixtures. The oxidation time at 0.5 vol % oxygen is long enough to permit thickness measurements of the first few monolayers. The initial slope of the growth curve is quite different from the region starting at about $t \geqslant 10$ Å, and changes again between 30 and 35 Å. A detailed explanation of these phenomena is not available.

It is interesting to note that RF cleaning of the surface of the base electrode with Ar accelerates the oxidation process. The higher the RF voltage during Ar cleaning, the thicker the oxide film, and the lower the current density, certainly due to increased surface damage by ion bombardment.

4.2 - Ion scattering spectrometry

Ion scattering spectrometry have been successfully used with low energy ions to study the surface of anodized niobium at Argonne [17]. Measurements are only sensitive to the surface monolayer and the depth profile is obtained by progressive sputtering of several hundred atomic layers. Helium ions are used for analysis and Ne ions for sputtering. The figure 2 represents the ratio of heights of the oxygen to niobium peaks for a 200 Å anodized Nb surface. The values of the ratio corresponding to Nb_2O_5, NbO_2 and NbO are reported on the figure.

An excess of oxygen is found near the surface, which is due to adsorbed gases (H_2O, CO, O). They are two plateau-regions with a relatively sharp transition, which correspond to Nb_2O_5 and NbO respectively; they are followed by a drop off into the bulk Nb metal. If the sputtering rates for Nb_2O_5 and NbO are identical, the thickness of the NbO layer could be estimated of about 80Å. But it is well known that the sputtering rate depends on chemical structure, and the values of 80 Å is only suggestive.

4.3 - Auger electron spectroscopy

A paper published by the Brookhaven group [8] reports AES measurements taken on Nb samples which were treated according to typical procedures used in the preparation of SC cavities, such as UHV degassing, chemical polishing, electropolishing and anodic oxidizing, in order to determine the oxygen depth profile of Nb surfaces.

Eigth Nb samples were machined from commercial reactor grade Nb. After surface treatment, the samples were stored in dry nitrogen and AES analysis was performed several weeks later. The UHV system in which the studies was carried out is capable of reaching 10^{-9} Torr. To obtain the depth profiles, surface layers are etched off by sputtering with Ar ions, with a residual Ar pressure of about 5×10^{-5} Torr in the system. The Auger spectrum are obtained while sputtering. Due to the large sputtering ion currents, which may create surface roughness and induce parasitic chemical reactions, the depth resolution was poor, and interpretations of the experimental data must be considered semiquantitative in character. Concentrations of O_2 below the at% level were not measurable.

Auger spectra from a clean Nb surface are obtained after removal of about 500 Å by argon sputtering.

In furnace cleaned samples, the region of high oxygen concentration is about 75 Å thick - in contrast with previous results [18] obtained from samples

cleaned in UHV and never exposed to air prior to the Auger analysis, which report an oxygen-rich region of only 10 Å at the Nb surface.

For chemically polished samples, oxygen penetration depth attains 100 to 150 Å, and after dissolution of oxide in acid, remains equal to about 90 Å. In addition, the various surface treatments correspond to different oxides: chemical preparations of Nb surfaces result in lower oxides than anodizing and than treatment at high temperature in UHV . In both cases, the oxide layer is made of pentoxide.

Concerning oxygen, the most significant conclusion to be drawn from this work is that the surface treatments result in surfaces covered by layers of lower oxides on the order of 100 Å thick. A typical Nb surface would have a layered structure consisting of a good dielectric pentoxide superficial layer, a two-phase (NbO_2 + NbO) layer, up to 50 Å thick; a two-phase layer NbO-Nb roughly 50 Å thick, followed by single phase Nb with O as interstitial.

4.4 - Auger electron spectroscopy and XPS

Very recently, at Karlsruhe [19], quantitative measurements of the oxidation of Nb surfaces have been carried out for typical procedures used in the preparation of Nb surfaces; UHV annealing, oxipolishing (OP), electropolishing (EP), handling in air, H_2O or H_2O_2 .

Measurements are performed in a X-ray photoelectron spectrometer with a base pressure in the 10^{-9} Torr region. After chemical treatment, or oxipolishing, or electropolishing, the samples are thoroughly rinsed in distilled water and dried in methanol before their transfer into the vacuum chamber. So they are in contact during about half an hour with air before starting to pump the vacuum tank.

Nb double peaks were used for the measurements. Double peaks for Nb, and Nb^{5+} ions in Nb_2O_5 are shifted by about 5.2 eV respectively, as shown on the figure 3. By a mathematical treatment of the observed peaks, it has been possible to obtain the contribution of the lower oxides. The measurement of photoelectrons at different angles of emission gives, in addition, the oxide thickness.

In all cases, the predominant oxide is Nb_2O_5. From the XPS spectra, the contribution of lower oxides may be obtained and then separated into contributions of two different valences, with two chemical shifts, one of which corresponds to NbO, the other being attributed to Nb_2O . It is important to emphasize that within the detection limit of the spectrometer, estimated to about one half a monolayer, NbO_2 was never present in the oxide coating.

The pentoxide layer is about 22 and 15 Å for OP and high temperature treatment (HT) respectively, with local variations of about ± 10 % . In contrast, EP samples are covered by a very rough pentoxide layer, whose thickness ranges from 70 to 390 Å. In all cases the mean thickness of lower oxides corresponds to about two monolayers, in contradiction to the results obtained by Hahn and Halama (50 Å).

Depth profiles measurements have been performed, with XPS and AES, by sputtering the oxides, in order to compare the results given by the two methods.

XPS results show that sputtering and electron bombardment are able to create in situ lower oxides. After one minute of Ar ion impact Nb_2O_5 has disappeared and only NbO is left on the surface.

Depth profiles obtained by AES are similar to those published by the Brookhaven group, the O content extending to a depth larger than the initial oxides thickness. A region of "dissolved" oxygen exists below the NbO layer, its extension being different for the various preparation methods. (From 20 to 40 Å for HT samples, up to 100 Å for EP and anodized samples).

XPS and AES allow the following picture of the Nb-Nb oxide interface, which is summarized on the figure 4. The formation of oxides on Nb starts with a metallic oxide, whose thickness has strong local variations, with a mean value of about 10 Å. On top of this NbO layer, an amorphous dielectric oxide Nb_2O_5 is growing. For Nb_2O_5 grown slowly, its external surface is very smooth. After cool-down in the furnace, and transfer to the XPS set up, Nb_2O_5 has a thickness of 20 Å, growing to about to 60 Å further in air in some weeks. For fast grown oxides (in H_2O or in H_2O_2), after some minutes a thickness of 60 Å is reached, with strong thickness variations. In addition, underneath the NbO layer, the Nb lattice contains dissolved oxygen, which is present partly as a bulk impurity, and partly due to the oxidation of the Nb surface.

As it will be shown later, NbO_2 may appear under electron bombardment, by picking up O from the residual atmosphere in the spectrometer.

4.5 - U.V. photon spectrometry (UPS)

The electronic structure of the valence band of Nb has been studied by ultraviolet photoemission spectroscopy (20), for a better understanding of the superconducting properties of these material, which is the element with the highest critical temperature. Furthermore, the highest T_c are obtained with compounds containing Nb.

Photoyield and energy distribution curves were obtained from Nb films evaporated onto a Nb substrate in a UHV chamber with a base pressure in the 10^{-11} Torr range. There is a good agreement between theory and experiment both concerning d-band width and structures in the valence band. Nb shows interesting surface properties, and is extremely sensitive to contamination. As an example, there is noticeable change in the EDC three hours after an evaporation despite the fact that the ambient pressure is better than 1×10^{-10} Torr.

The initial stages in the oxidation of Nb have been studied by the same UV photoemission technique, for photon energies below 12 eV .

Changes of structure in the electron distribution curves obtained in UPS are correlated with formation of different types of Nb oxides. At least three different oxides, or mixtures of oxides have been observed. NbO_2 and NbO oxides seem to form first a protective layer. The pentoxide Nb_2O_5 is obtained after heavier oxidation.

The first experiments were carried out at room temperature.

Except for the appearance of a peak corresponding to initial energies located 4 eV below the Fermi level with increasing exposure to oxygen, the initial increase in work function from 4.3 to 5.5 eV is the most remarkable

change. The fact that the work function then remains stable from 20 L to at least up to 10^4 L exposure indicates that the Nb surface is passivated very quickly due to the formation of a thin protective oxide layer. From the evolution of the shape of the energy spectrum it is clear that this layer is metallic in character.

When the oxidation is performed at elevated temperature, the protective layer may be broken up and a new oxide is formed, probably NbO_2 . If the samples are oxidized at high temperature, and atmospheric pressure, the energy distribution curves become progressively characteristic of an insulator, probably Nb_2O_5 .

The figure 5 represents the different oxidation stages for Nb.

Other experiments on oxidation of Nb and Nb_3Sn were performed using thin foils of Nb and photons with higher energies ($h\nu \geqslant 100$ eV), in a UPS equipped with an AES (21).

A successful method for obtaining atomically clean Nb surfaces is described:

- an heating to temperatures greater than 2000 °C in UHV with $p \simeq 10^{-9}$ Torr for 15 minutes evaporates off Nb oxides,
- temperature is then lowered to 1400 °C for 15 minutes, to allow carbon to diffuse from the surface to the bulk,
- finally, the surface must remain at about 800 °C, prior to measurement, to prevent a chemisorption of O_2 or CO .

With this procedure, contamination free AES and UPS spectra are obtained.

In these experiments, chemical shifts of the peaks have been measured, and their observation confirms the existence of three stages in the oxidation processes, corresponding to the formation of the distinct Nb oxides: NbO, NbO_2 and Nb_2O_5 . The oxygen would initially diffuse into the bulk, forming a NbO layer. The NbO layer continues to grow deeper into the bulk and a new NbO_2 oxide nucleates at the surface. These new layer also propagates into the bulk material as the Nb_2O_5 nucleates at the surface. Finally, a Nb_2O_5 layer grows into the bulk and perhaps a mixed phase of NbO_2 remains included in the Nb_2O_5 as it grows. At room temperature, and with 10^3 LO_2 exposure the oxide grows deeper than the escape depth at 21.2 eV in the Nb_2O_5 (which is about 20 Å).

In a second serie of experiments, clean and oxidized Nb_3Sn surfaces were studied using photoemission spectroscopy, to determine valence and core levels. For clean Nb_3Sn, the valence band bears a strong resemblance to Nb.

The first stages of the oxidation of Nb_3Sn were also studied. Compared to Nb, the oxides of Nb_3Sn form a protective layer, but the oxygen penetration is not as deep - as shown by the energy spectra corresponding to a metallic emission, even for near the saturation. In the higher energy data, chemical shifts of the peaks can be associated with SnO_2 and Nb_2O_5, in addition to Nb_3Sn or Nb metal and other Nb oxides. After annealing the sample to 1000 °C, the outer layer of the oxide is composed essentially of SnO_2 and Nb_2O_5, with a thickness of about 10 - 15 Å, that is less than for pure Nb.

V. IRRADIATION EFFECTS

Electron irradiation effects on oxidized Nb foils and Nb_2O_5 was studied by AES [22]. From observed shift of the energy peaks, one is able to examine the beam effect on the specimen. The figure 6 represents two series of Auger spectra recorded from an oxidized Nb foil, bombarded by electrons of energy E_p = 2 keV and with a current I_p = 15 μA and from a pure Nb_2O_5 powder as a reference. In a spectrum corresponding to oxidized Nb, the transition peaks involving valence electrons appear to be doublet, the separation of each doublet being about 5 eV . The low energy peak in each doublet exists only in the oxide state, and corresponds to Nb atoms bound to oxygen. The other peak is the "metal" peak. By irradiation, the metal peak grows at the expense of its oxide counterpart and in the meantime the oxygen peak height reduces correspondingly. The surface of the oxidized sample becomes enriched with Nb due irradiation-induced dissociation of the oxide, and loss of oxygen. At the same time, the carbon peak shape remains graphite-like in form, indicating that no carbide builds up under electron bombardment.

The beam irradiated region, on both type of specimens, can be easily recognized by a colour change: the white colour of the Nb_2O_5 powder decreases and the dark colour of metallic and lower oxide (NbO) mixture increases by bombardment.

The observation of dissociation and reduction of surface oxide was supported by ESD measurements, by measuring the H^+, OH^+ and O^+ signals with a quadrupole mass analyzer. A sharp increase of the O^+ signal is observed in the earlier stages of electron bombardment. After 5 h of bombardment, O^+ dominates the final ESD spectrum. (ESD = Electron Stimulated Desorption).

A careful analysis of the observed Auger peaks leads to the conclusion that the superficial layer of an oxidized Nb foil was enriched with about 50 % of Nb, due to beam irradiation, the altered layer being more than 100 Å thick.

These observations clearly show that the electron beam can greatly alter the composition of the Nb oxide, under particular conditions and some precaution must be taken when using a combination of AES and simultaneous ion sputtering, since the sputter-etch rate can increase within the illuminated beam area.

The action of electron irradiation on thin Nb oxides have been studied independently by XPS [19], after impact of 1 keV electrons with a density of 100 μA/cm^2. With irradiation, the oxide NbO_2 appears and grows till about 3 monolayers in 70 minutes; at the same time, the Nb_2O_5 intensity decreases and the oxygen concentration in the metal slightly increases. No change can be observed in the region of lower oxides.

If higher current densities are used in the electron beam, the NbO_2 signal shrinks and the Nb_2O_5 signal grows, because O is picked up from vacuum, in agreement with our observations [23].

Thus, the electron beam action may be very different, depending on the experimental conditions, and most particularly on current density and residual atmosphere composition.

The action of low energy ions have been observed in the same experiments: after Ar sputtering with 1 kV ions (2.5 μA/cm^2) Nb_2O_5 disappears and a lower oxide (NbO) is created by the ion bombardment, which extends to a depth larger then the initial oxide thickness.

In addition, Ar ion bombardment change the line shape of the carbon signal from graphite (hydrocarbons) to carbide.

The bombardment of Nb_2O_5 with Kr^+ or O_2^+ ions also leads to the development of a surface layer of NbO [24]. The layer begins to form at 3.4×10^{15} ions/cm^2 as random nuclei of diameter 10 to 15 Å which can be resolved by transmission electron microscopy. The final thickness of the surface layer is roughly 300 Å. In these experiments, Nb_2O_5 films were peeled off from oxidized Nb plates, then supported on grids and bombarded by 35 keV ions. The bombarding current was kept to about 5 μA/cm^2 to avoid thermal heating. High energy electron diffraction gives patterns which are characteristic of NbO .

This phenomenon can be understood from a model which combines preferential oxygen sputtering at the surface, diffusion of the relevant point-defects and random nucleation of the suboxide NbO . A gradual colour change from white to black was observed during bombardment with darkening complete at a dose of about $1-3\times10^{17}$ ions/cm^2.

Irradiation of Nb and oxidized Nb surfaces by high energy ions in superconducting cavities has led to contradictory results. At Brookhaven [25] irradiation by high energy protons lead to an heavy degradation of Q and RF peak field values, the anodized cavities showing a considerably greater degradation that those not anodized. On the contrary, experiments carried out in the Siemens laboratory on anodized cavities after irradiation by 1 or 3 MeV protons, were unable to show any influence of the irradiation upon the Q and the peak magnetic field [26].

In the Siemens experiments, the whole cavity was homogeneously irradiated, and the calculated density of defects produced in Nb were 10 - 100 times greater than that obtained at Brookhaven. At Brookhaven, only an area of 1 cm^2 was bombarded with protons.

It is suggested that the observed degradation is not due in any way to the formation of lattice defects in Nb.

Considering now the action of ions on the oxide, lower oxides are certainly formed by reduction of Nb_2O_5 . But again, the total energy dose in the oxide is 10 to 100 times greater in the second serie of experiments. In conclusion, Nb_2O_5 seems to have a high resistance to radiation.

From various experiments performed with ion bombardment, we may conclude that ion bombardment creates lower oxide (NbO, NbO_2) by reduction of Nb_2O_5, and progressively transforms a smooth surface into a rough surface. Surface damages certainly accelerates the oxidation of Nb surfaces, O being taken from the residual atmosphere, and an equilibrium between sputtering and readsorption of oxygen may be observed. All these phenomena explain that in the depth profiles obtained by AES, the O content extends to a depth larger than the true oxide thickness.

Thus by combining AES (or ISS) and ion sputtering it is difficult to obtain the real composition and distribution of oxides in the surface layer. Only relative comparisons between profiles of differently prepared samples can be made by this destructive methods. Only XPS, UPS, without ion sputtering will be able to give quantitative results - but only for very thin surface layers -.

PART II. ELECTRON EMISSION

I. INTRODUCTION

One of the principal limitation in achieving high accelerating fields in microwave cavities is the phenomenon of multipactor. In Nb cavities operating in S-band, studies at Stanford, Cornell, Karlsruhe and Wuppertal, have shown that one surface multipactor is the dominant limiting mechanism.

Resonant multiplication may take place provided that the secondary emission coefficient of the surface is larger than unity. According trajectories calculations, in cylindrical or in rectangular muffin-tin cavities, the electrons return to the surface with kinetic energies in the 50 - 1000 eV range, and it is clear that the secondary emission coefficient in this primary energy range plays a crucial role in determining the strength of the multipactor barriers.

Several laboratories have measured the secondary emission coefficient for materials of interest to superconducting accelerators cavities, the surfaces of the samples being prepared by the methods commonly employed for superconducting cavities.

At Cornell University, the material tested were Nb, anodized Nb, Nb_3Sn, NbN, Ti and TiN . These two last materials have been deposited in the past as coating for surfaces of conventional microwave copper cavities in an attempt to suppress multipactor, and more recently on Nb cavities.

At Paris, we have measured Nb, oxidized Nb, Cu, and thin layers of Ti and C deposited on Nb.

At CERN, a systematic study of the influence on secondary emission from Nb of various surface treatments have been recently carried out.

The influence of thin oxide layers on the secondary emission has been studied at Karlsruhe.

2. SECONDARY EMISSION FROM Nb SURFACES

In the Cornell experiments [27], the sample were placed in a UHV system pumped out to 10^{-9} Torr, and the area under test was cleaned by ion sputtering. An Auger spectrum was registered immediately after.

Values of δ are given as a function of primary electron energies E_p, that are varied from 200 to 2000 eV, for surfaces in typical situations: before cleaning, after cleaning (i.e. after removal of a 200 Å thick layer by ion sputtering) and finally after exposition to air (Fig. 7).

For a clean Nb surface, δ_{max} attains about 1.2 and the energy domain $E_1 < E < E_2$ in which δ is greater than unity extends from about 100 to 1300 eV. After cleaning, the secondary emission from Nb covered with a 2000 Å thick layer of Nb_2O_5 , is lower than the one from clean Nb . Before cleaning, the emission is comparable in both cases. But Nb_2O_5 reduces the width of the energy domain $E_1 - E_2$ to about 150 - 800 eV. In all cases, an exposure to air increases the secondary emission yields.

Auger spectra show that in pure Nb, a carbon peak is always present, even after cleaning. In Nb_2O_5 the carbon peak is present before cleaning, disappears after ion sputtering, and slightly reappears after an exposure to air. Nb_2O_5 is always contaminated by nitrogen, due to the NH_3 bath.

These results for Nb and anodized Nb suggest that cavities surfaces prepared by wet chemical methods are likely to show strong multipactoring, but that the situation may be improved by an argon discharge, cleaning the contaminated surfaces in situ.

Secondary emission from clean Nb_3Sn may be compared to the emission from clean Nb, with a δ_{max} of about $\delta_m = 1.3$

The new material NbN ($T_c \simeq 16\,K$) has a secondary emission coefficient larger than unity, and the curve $\delta(E_p)$ is quite close to the curve corresponding to Nb_2O_5.

Clean Ti would be a very interesting material, as its δ coefficient remains lower than unity ($\delta_m \simeq 0.95$), but unfortunately, an exposure to air markedly increases δ_{max} to about 1.35 . In comparison the emission of a thin layer of TiN, 1000 Å thick, obtained by reactive sputtering of Ti in a N atmosphere, is larger that the emission from Ti before cleaning, with $\delta_m \simeq 1.5$, similar after cleaning ($\delta \simeq 0.95$) but is less severely affected by an exposure to air (Fig. 8).

This suggests that TiN may prove a more favourable coating than Ti for the suppression of multipactor, at the condition to prepare the material in situ and then avoid subsequent contamination.

Having in mind these results the Cornell group attempted to determine how the RF performances of SC cavities can be affected by applying thin coatings of similar materials, as well to try to overcome the multipactor barriers [28].

Single cell X-band and S-band muffin-tin cavities have been coated. Before coating the Q_o factor of S-band cavities lie between 5×10^9 and 1.5×10^{10} . At high RF power, multipactor barriers were encountered between 4 - 5 MeV/m and 7 - 10 MeV/m . Very thin coatings films (150 - 300 Å) of Ti, TiN and Rh, have been deposited on the walls of the cavities. Of these three materials, Ti has the most pronounced effect on Q_o while TiN has the least. The presence of a normal metal film increases the surface resistance but does not create hot spots at high power, so that fields up to 8 MeV/m can still be realized. Unfortunately the multipactoring behaviour remains unaltered by Ti, and adversely affected by TiN . Only the rhodium coatings appear to have beneficial effects, and this may perhaps be related to the absence of any significant oxide layer. In addition, it is not sure that the very thin films used in these experiments were continuous, and that Nb islands with high values of δ were not present.

At CERN [29], various aspects of secondary electron emission have been recently studied, in order to explain the influence on the secondary emission coefficient δ of (i) the surface treatment, (ii) the electron dose, (iii) the angle of incidence of the primary electrons, and (iv) the temperature.

Concerning the surface treatment, the conclusions are the following:

- baking the vacuum chamber containing the sample at 300 °C during 24 hours decreases δ. After this treatment, a short exposure to the air increases slightly δ without recovering the initial values of the emission.

- electropolishing seems to have a weak influence on δ, which decreases only at high primary energies.

- a gaseous discharge in Argon at a pressure of 10^{-2} Torr, with an ion dose of about $10^{18}/cm^2$, the ion energy being 1 keV, decreases δ by a large factor. The figure 9 shows the curves corresponding to an unbaked surface, and to a baked surface after cleaning by gas discharge.

If the gas discharge cleaning is performed in an unbaked system, the secondary emission of the cleaned surface is instable, and δ increases slowly with time. On the contrary, if the discharge cleaning takes place in a baked system, the emission coefficient has low and stable values.

- the influence on δ of the electron dose is in good agreement with our results (30).

- if a baked surface is cooled to 4.2 K, the values of δ are the same that the values obtained at ambient temperature before cooling (see Fig. 10).

Auger spectra show that after a gaseous discharge, the carbon and oxygen peaks disappear. The ion bombardment seems to sputter the oxide layer, and also the Nb layer containing adsorbed oxygen. The total absence of carbon is surprising, as carbon is present in the original sample, but we may assume that carbon is eliminated by the discharge, after a chemical reaction with oxygen, like in an outgassing process at high temperature. After an electron bombardment with a dose of about 1.2×10^3 C/cm^2, carbon and oxygen peaks are again present in the Auger spectra. Electron bombardment is at the origin of a chemical transformation of a surface, after induced adsorption of molecules from the residual atmosphere.

Very important results have been obtained concerning the evolution of the parameter E_1 and E_2 which characterize the two electron primary energies for which $\delta = 1$, for various conditions: (i) for an unbaked surface, E_1 is less than 30 eV; (ii) after baking and gas discharge, E_1 is raised to 140 eV, and δ_m lowered from 2.5 to 1.23 ; (iii) an exposure to air during 8 hours lowers E_1 to 34 eV, and a new bakeout increases E_1 till 100 eV ; (iv) a new discharge will be necessary to recover the preceding value of $E_1 = 140$ eV .

A gas discharge in Argon seems a good method to clean the surface and to suppress high order barriers of multipactor, by rising the values of E_1 .

III. ACTION OF THE ELECTRON BEAM ON SECONDARY EMISSION

The first experiments made in our laboratory to study the secondary emission of various metal surfaces in 1977-1978 have pointed out the strong influence of the electron bombardment on the evolution of δ. For these experiments, a vacuum chamber with a residual pressure of about 10^{-8} Torr was used.

For all specimens (Nb, oxidized Nb, Cu, Au) cleaned in methyl alcohol before their introduction into the chamber, it was observed a rapid decrease of δ during the first 10 or 20 minutes of bombardment (Fig. 11 (a)), the de-

creasing-rate being approximately proportional to the electron dose. For Nb, or Cu, which are always covered by a native oxide layer, the initial decrease of δ is followed by a slow increase, and after several hours, a stable value of δ is attained. This value increases if the sample is exposed to air, in agreement with Cornell and CERN experiments.

If the sample is coated by a Nb_2O_5 layer 400 to 1000 Å thick, δ decreases continuously towards its final value, with $\delta_m \simeq 1.05$ (Fig. 11 (b)).

Some experiments have been carried out in an Auger electron spectrometer with imaging possibilities. The bombardment regions of the Nb samples were visible on the screen, and analysis of bombarded and unbombarded regions gave different results: the oxygen peak is higher in the irradiated zones, and the carbon peak lower, than in the surrounding regions.

The chemical action of the electron beam is particularly strong on a clean copper surface, covered by its natural oxide layer. A few seconds of bombardment with a current density of about 1 mA/cm^2 is sufficient to change the colour of the bombarded area from red to purple corresponding to the growing of a dielectric layer, probably made of Cu-oxide. At very low electron dose, the irradiated region is not visible in high vacuum, but if the sample is exposed to air, the purple colour appears slowly, and the superficial oxide layer grows continuously during days.

Such a visible phenomenon was not observed with Nb or Nb_2O_5 surfaces, contrasting with other experiments [22]. The composition of the residual atmosphere in the vacuum chamber that differs in the respective experimental devices, certainly plays an important role.

More recently, experiments were performed in a better vacuum (3×10^{-10} Torr) after outgassing the vacuum chamber at 300 °C during 24 hours [31]. The evolution in time of δ was shown to be more rapid than in previous experiments, made at a pressure about 10^{-8} Torr. In the new system, the primary electron energy has been varied from 50 to 2500 eV. The limit value of δ under bombardment is the same in both cases for Nb surfaces.

Several thin film coatings were studied: Ti and C. Very thin films of both materials have an important action on the emission, and δ_m decreases to values lower than unity for a Ti film thickness of about 100 Å. (Fig. 12).

Carbon film, obtained by evaporation from high purity carbon electrodes, have a curve $\delta(E_p)$ which strongly differs from the metal curves. The region with $\delta > 1$ is reduced more and more by the electron bombardment, but without rotation of the initial linearly growing part of the curve. The energy corresponding to $\delta = 1$ is only 200 eV, and the peak in $\delta(E_p)$ becomes sharper and sharper by increasing the layer thickness (Fig. 13). Values of $\delta_m < 1$ are obtained with a thickness of about 100 - 150 Å.

IV. INFLUENCE OF A THIN OXIDE LAYER ON SECONDARY EMISSION

In order to explain the influence on the secondary emission yield of the oxide layer, and of the adsorbates, that always cover Nb - or Nb_3Sn - surfaces, and also the variation of the emission induced by electron or ion impact, experiments have been carried out at Karlsruhe, by X-ray photoelectron spectroscopy [19][32]. The "secondary electrons" that are measured, are slowed-down photoelectrons.

It can be shown that the true secondary electrons produced by electron impact are proportional to the "secondary electrons" created by X-rays, and because the shape of the curve giving δ as a function of the primary electron energy E_p is universal for homogeneous materials, it may be assumed that the electron current measured in X-ray experiments is directly related to the maximum value δ_m of δ. Thus only variations of δ_m are reported, for various surface treatments, and in relation with the chemical composition of the oxide layer. XPS shows that homogeneous layers of Nb_2O_5 are found for dry oxides (obtained by H.T. treatment of Nb) about 20 Å thick, whereas wet oxides (obtained by oxipolishing, electropolishing, or washing in water) are thicker (about 60 Å) and inhomogeneous. Wet oxides contain adsorbed H_2O molecules and all oxides may contain adsorbed hydrocarbons or CO_2 on their surface.

Wet oxides are positively charged by irradiation with X-rays, and this positive d.c. charging enhances electron emission by lowering the work function. On the contrary hydrocarbons become negatively charged, enhance the work function and then lessen the secondary emission.

Large variations of secondary emission observed during electron - or ion - bombardment may be explained at least qualitatively by taking into account both types of adsorbates, and the charge variations at the oxide surface. In addition, electron bombardment has a strong chemical action on the oxide itself and on the adsorbates. With electron impact the main change for the O-adsorbates (H_2O, O) is the transformation of Nb_2O_5 into NbO_2, the growth of the oxide at the expense of the adsorbate and of the residual atmosphere. For the C adsorbates (CO, CO_2, CH_3OH, oil molecules), polymerization may be induced by the electron beam.

Namely, δ_{max} is enhanced over δ_{max} relative to clean Nb by 30 % for dry Nb_2O_5, by 50 % for Nb_2O_5 containing chemisorbed water molecules, and strongly reduced if hydrocarbons present on the surface are polymerized by the electron beam.

Water adsorption and O-adsorbates may be eliminated by heat treatment or by helium or ion processing, thus reducing δ.

With oxide containing hydrocarbons, δ decreases of about 40 % for an electron dose around 1 C/cm^2 . At Paris or at CERN, variations of 30 and 40 % respectively were found for an electron dose of 10 C/cm^2 with oxides having a different composition, and also the residual atmosphere was different.

From this work, it is suggested to reduce the secondary emission by covering the surface with very thin films of polymerized hydrocarbons, which would give lower emission than Nb_2O_5 oxide layers, but it will be a difficult task to elaborate stable layers in situ, and avoid the contamination of their surface. It seems more realistic to cover the surface with a thin carbon film.

V. FIELD EMISSION

At very high field levels, loading and X-ray emission which result from field emitted electrons also limit the field level that can be achieved in practice in SC cavities.

Field emission experiments at helium temperature have been performed at Stanford (HEPL) both for d-c and RF fields in order to study field emission enhanced by resonant tunneling of electrons through surface-states associated with adsorbed atoms (33).

Field emission from clean surfaces occurs at values of the field greater than 3×10^7 V cm^{-1}, as shown by experiments with a point cathode facing a plane anode.

Field emission between broad area electrodes occurs for field values 10 to 100 times smaller than this and currents are observed which are many orders of magnitude greater than those predicted by the Fowler-Nordheim law. These apparent discrepancies between systems utilizing point-to-plane geometry and systems using broad area electrodes are easily explained by the existence of microscopic projections on the surface of large electrodes, even after polishing. On the tip of these micropoints, the local field may be enhanced by a factor β greater than 10^2, compared to the mean field existing between the electrodes. In addition, the anomalous behavior of the emitted current may be due to the presence of adsorbed atoms on the surface, which introduce a potential well in the potential barrier. If bound states of the adsorbate are slightly under the Fermi level, resonant tunneling of electrons from the metal to the vacuum increases dramatically the current, as the transition probability of electrons of energy equal to the adsorbate level is greatly enhanced. Experimental measurements of the energy distribution of emitted electrons demonstrate the existence of this resonant tunneling process.

Using the point-to-plane geometry, enhancement factors of 10^3 to 10^4 for the emitted current are easily observed between a very clean tip surface and a tip covered with adsorbates (Fig. 14).

Processing techniques can be applied in cavities to reduce field emission. As an example, a low current glow discharge in helium at a pressure of 10^{-4} Torr, has two specific actions on the surface: destruction of the emitting micropoints having the maximum field enhancement factor, and desorption of the atoms bound to the metal - or to the oxide surface.

In cavities, at high field levels, field emitted electron can be accelerated to high energies, and X-rays are produced. The variation of the intensity of X-radiation as a function of the peak electric field in the cavity are in good agreement with theory, assuming field electron emission from the wall. Helium processing at relatively low power level during hours, is able to reduce X-ray emission by large factors and consequently to increase the power injected in the cavity. A careful study of the influence of the processing on the emitted X-ray radiation led to the conclusion that sputtering of adsorbed atoms takes place in the earlier stages of processing, corresponding to a lowering of the apparent field enhancement factor β, and an increase of the work function. From these experiments, the factor β cannot be considered only as a geometrical factor, but like a fitting factor, as pointed out by Halbritter [34].

In Nb cavities, the local RF field is enhanced at geometrical protrusions by a factor β of about 200, for cleaned surfaces. After adsorption, the values of β calculated from FN plots may be as high as 500 - 600. This apparent increase of β may be explained in terms of resonant tunneling.

Finally the reduction of field emitted electrons currents, that was observed in microwave cavities by rising the frequency from S-band to X-band may be also explained by a reduction of the apparent β factor, due to the finite transit time of the electrons through the oxides and a reduced positive charging of the surface [34].

Large area Nb electrodes were also used in experiments carried out at He temperature at Orsay [35], in order to study the influence on the field emitted

electron current of the thickness of a Nb_2O_5 coating. No ion processing was made in the d.c. experimental diode, but a measure of the temperature increase of the cathode on the order of a few K, show that this electrode is permanently bombarded by ions created by the electrons hitting the anode and stimulating the desorption of gaseous species. After a few hours, the I.V. characteristics of the diode are stable enough to obtain reproducible results.

It was shown that an increase of the Nb_2O_5 thickness from zero (Nb + natural oxide) to 1600 Å decreases the current by several orders of magnitude (Fig. 15). At the same time the apparent enhancement factor remains nearly constant, between 150 and 200 for oxide thicknesses ranging from 50 to 400 Å. For thicker oxides, β decreases and reaches 60 - 90 for a layer thickness of 1600 Å.

VI. DISCUSSION

A survey on electron emission phenomena from oxidized metal surfaces by Halbritter was, at the same time, an attempt to explain the great number of observations mode in various laboratories, which often were in contradiction and not- or misinterpreted. [35].

The basis for a satisfying explanation was found later [32] in the presence or the absence of electric charges in the outer atomic layers of the oxides - or in superficial adsorbates. These charges can be induced naturally be the adsorption of atoms - as mentioned earlier - but also by electron or ion bombardment, and by electron secondary emission under X-ray or electron bombardment. The sign of this charges depends on the chemical composition of the adsorbates and on the energy of the bombarding particles. As an example, for very low or high electrons energies, the secondary electron emission coefficient is less than unity and the surface becomes negatively charged. On the contrary, for δ greater than unity, the oxide surface becomes positively charged.

The conduction of electrons through the Nb oxide layer results from two phenomena: field emission from the metal to the conduction band of the oxide, which is for Nb_2O_5 very close to the Fermi level, and also hopping conduction through impurities levels located in the forbidden band, and from this levels to the conduction band.

The electric field applied to the metal surface has two origins: the external field, shielded by the high dielectric constant of the Nb_2O_5 oxide ($\varepsilon \simeq 30$), and essentially the short range action of the charges existing on the oxide surface.

For these reason, positive charges distributed on the surface may be considered as "holes" in the potential barrier, when an high external field is applied normal to the surface (Fig. 16), and the field emission is dramatically enhanced. This phenomenological model is equivalent to the quantum mechanical resonant tunneling model.

If now an electron bombardment is able to create superficial positive charges - as an example by ionizing oxygen vacancies which originally contains two electrons - the energy diagram is locally distorded, and even without an external field, electrons are emitted, leading to a local value of δ which may attain values as high as 100 or 1000 ; as a consequence, the mean value

of δ over the whole surface increases. This phenomenon was in the past called "Malter effect". Only the electrons injected from the metal into the conduction band of the oxide are able to pass over the potential barrier.

Conversely, negative charges on the surface locally reduce the secondary emission. It was the case for carbon or hydrocarbons adsorbates, and graphite layers deposited on the surface.

For thicker and thicker oxide layers, the distance between the Fermi level and the conduction band of the oxide increases rapidly, thus reducing the tunnel current flowing from the metal to the conduction band and consequently, decreases the field emitted current.

Another consequence of the presence of positive charges in the oxide layer on Nb surface is the lowering of the apparent work function of the surface, and the enhancement of the apparent field factor β, which increases the field emission.

As far as secondary emission is concerned, evolution of the secondary emission coefficient under electron bombardment towards lower values may explain the observed possibility to overcome multipactor barriers of high order, the multipacting discharge decreasing in intensity with time and finally die out.

Experiments on the lowering of δ_m towards values less than unity by deposition of thin films have to be continued. From the Cornell work, one might be tempted to try thicker coating of Rh, or perhaps Au, about 500 Å thick, in order to obtain a continuous layer and a complete coverage of the underlaying Nb . It is conceivable that the RF losses in such a thick normal metal coating might be lessened by the superconducting proximity effect.

Our experiments with carbon films are encouraging, as carbon may lower δ_m to $\delta_m < 1$, and considerably decreases the $E_1 - E_2$ domain for which $\delta > 1$, before bombardment. The influence of C under a graphite form is in agreement with the suggestion by Halbritter to cover the surface with hydrocarbons films. It will be now necessary to measure the surface resistance of carbon covered Nb surfaces, and to attempt to suppress multipacting barriers in real cavities by using thin carbon coatings.

The CERN work demonstrates the important effects on δ and on the $E_1 - E_2$ domain of (i) a thorough outgassing before cooling the surface, (ii) a very low residual pressure ($\simeq 10^{-10}$ Torr) and (iii) ion cleaning by an argon discharge. Such a ion processing is well known to decrease dramatically the field emission currents. Adsorbed nitrogen is known to lessen field emission, and could certainly be used for ion processing. From the experiments at IBM [16], nitrogen gives better results for cleaning a Nb surface. A careful study of the influence of ion processing by a discharge in nitrogen on secondary and field emission would be necessary.

Finally, we may emphisize that a decrease of the maximum secondary emission yield to values less than unity is not a necessary condition to avoid multipactor: it would be sufficient to obtain a yield less than unity for electrons energies corresponding to the energy spectrum of the electrons active in the multipacting process. For these reason, an evolution of δ in which the initial linear part of the curve giving $\delta(E_p)$ rotates clockwise under electron or ion bombardment will be highly favourable.

We suggest to coat the surface with thin layers of materials having their curve $\delta(E_p)$ displaced to higher energies than the homogeneous materials used till now. It is well-known that metals with high δ coefficients have at higher energies that metals with weaker values of δ_m. Surprisingly, following this reasoning, metals with a high value of δ_m, like Au or Pt, could be superior to others, as far as high order multipactor is concerned.

Another possibility would be to study emission coefficients of porous layers, that have emission properties very different from those of homogeneous layers.

REFERENCES

1 WERNER, H.W. - Modern methods for thin film and surface analysis. Mat. Sci. and Engng 42, 1980, p.1

2 BERANGER, G., D. DAVID, E.A. GARCIA, X. LUCAS - Etude de la contamination superficielle des métaux au moyen de la microanalyse nucléaire. Rev. Phys. Appliquée 10, 1975, p.87

3 PADAMSEE, H., J. KIRCHGESSNER, M. TIGNER, R. SURDELIN, M. BANNER, J. STIMMEL, L. PHILLIPS - Fabrication and performances of muffin-tin microwave cavities for accelerator use. Cornell University CLNS-340 and IEEE Trans. MAG 13, 1977, p.346

4 DICKEY, J.M., M. STRONGIN, O.F. KAMMERER - Studies of thin films of Nb_3Sn or Nb. J. Appl. Phys. 42, 1971, p.5808

5 UZEL, Y., B. HILLENBRAND, K. SCHNITZKE - Zur Preparation von Nb_3Sn Schichten auf einkristalliner Nb-unterlage. DPG, Fachausschuß Tiefe Temperaturen, Freudenstadt 1980

6 SUNDELIN, R., E. von BORSTEL, J. KIRCHGESSNER, D. RICE, M. TIGNER - 3 GHz SC accelerator cavity for use in an electron synchrotron. IEEE Trans. NS 20, 1973, p.98

7 HOYT, E.W. - Nb surfaces for RF superconductors. SLAC PUB 977, oct. 1971

8 HAHN, H., H.J. HALAMA - AES depth profile measurements of Nb for SC cavities. J. Appl. Phys. 47, 1976, p.4629

9 MAUREL, B., D. DIEUMEGARD, G. AMSEL - Nuclear study of the fluorine contamination of Ta by various polishing procedures and its behavior during subsequent anodic oxidation. J. Electrochem. Soc. 119, 1972, p. 1715

10 CHERKI, C. - Film-formation oxygen yield in the anodic oxidation of Nb. Electrochemica Acta, 16, 1971, p.1727

11 GIORDANO, S., H. HAHN, H.J. HALAMA, C. VARMAZIS, L. RINDERER - Influence of solute oxygen and nitrogen on SC Nb cavities. J. Appl. Phys. 44, 1973, p.4185

12 WILSON, P.B., Z.D. FARKAS, H.A. HOGG, E.W. HOYT - Recent measurements at SLAC on SC Nb X-band cavities.
SLAC PUB 1228, March 1973 and IEEE Trans., NS 20, 1973, p.104

13 DICKEY, J.M., H.H. FARRELL, O.F. KAMMERER, M. STRONGIN - Surface studies on Nb and some implications for superconductivity.
Phys. Lett. 32 A, 1970, p.483

14 STRONGIN, M., H.H. FARRELL, H.J. HALAMA, O.F. KAMMERER, C. VARMAZIS, J.M. DICKEY - Surface condition of Nb for SC RF cavities.
Particle Accelerators 3, 1972, p.209

15 KNORR, K., J.D. LESLIE - Ellipsometric measurements of the plasma oxidation of Nb and Ta and their interpretation.
J. Electrochem. Soc. 121, 1974, p.805

16 BROOM, R.F., R.B. LAIBOVITZ, Th. O. MOHR, W. WALTER - Fabrication and properties of Nb Josephson tunnel junctions.
IBM Journal, 24, 1980, p.213

17 GRAY, K.E. - ISS depth profile of anodized Nb.
Appl. Phys. Lett. 27, 1975, p.462

18 JOSHI, A., M. STRONGIN - Scripta Metallurgica 8, 1974 p. 413

19 GRUNDNER, M., J. HALBRITTER - XPS and AES studies on oxide growth and oxide coatings on Nb.
J. Appl. Phys. 51, 1980, p.397

20 LINDAU, I., and W.E. SPICER - Oxidation of Nb as studied by the UV photoemission technique.
J. Appl. Phys. 45, 1974, p.3720

21 MILLER, J.N. - Photoemission studies of clean and oxidized Nb and Nb_3Sn surfaces.
Ph.D. Thesis, Stanford 1980 (to be published in J. Appl. Phys.)

22 LIN, T.T., D. LICHTMAN - Electron irradiation effects on oxidized Nb foil and Nb_2O_5.
J. of Mat. Sci. 14, 1979, p.455

23 LAVAREC, M., P. BOCQUET, A. SEPTIER - Variation du coefficient d'émission électronique secondaire de surfaces réelles sous l'effet du bombardement électronique primaire.
C.R.Acad. Sci. Paris, 288 B, 1979, p.77

24 MURTI, D.K., R. KELLY - Preferential oxygen sputtering from Nb_2O_5.
Thin Solid Films, 33, 1976, p.149

25 HALAMA, H.J. - Effects of radiation on surface resistance of SC Nb cavity.
Appl. Phys. Lett. 19, 1971, p.90

26 MARTENS, H., K. WHOLLEBEN -
Irradiation of SC cavities with protons.
Phys. Lett. 42 A, 1973, p.393

27 PADAMSEE, H., A. JOSHI - Secondary electron emission measurements on materials used for SC microwave cavities.
J. Appl. Phys. 50, 1979, p.1112.

28 PADAMSEE, H., M. BANNER, M. TIGNER -
Suppression of multipactoring in SC cavities.
IEEE Trans., NS 24, 1977, p.1101

29 HILLERET, N. - Influence of surface treatment, electron dose, and temperature on secondary emission from Nb surfaces.
1980 - Private communication.

30 LAVAREC, M., P. BOCQUET, A. SEPTIER -
Lowering of the secondary electron emission coefficient of real surfaces due to the primary electron bombardment.
Proc. 8th Int. Symp. on Discharges and Electr. Insul. Vac., Albuquerque, 1978, p. C 3-1.

31 NGUYEN TUONG Viet, G. SAYAG, A. SEPTIER -
Secondary emission from Ti and C thin films on Nb.
(unpublished).

32 GRUNDNER, M., J. HALBRITTER -
On surface coatings and secondary yield of Nb_3Sn and Nb.
J. Appl. Phys. 51, 1980 (to be published)

33 SCHWETTMANN, H.A., J.P. TURNEAURE, R.F. WAITES -
Evidence for surface state enhanced field emission in RF SC cavities.
J. Appl. Phys. 54, 1974, p.914

34 HALBRITTER, J. - On electron emission phenomena from oxidized metal surfaces. Their application to electron loading in Nb high frequency cavities.
KfK Ext. 3/781, 1978

35 SAYAG, G., NGUYEN TUONG Viet, H. BERGERET, A. SEPTIER.
Field emission from oxidized niobium electrodes at 295 and 4.2 K .
J. Phys. E 10, 1977, p.176.

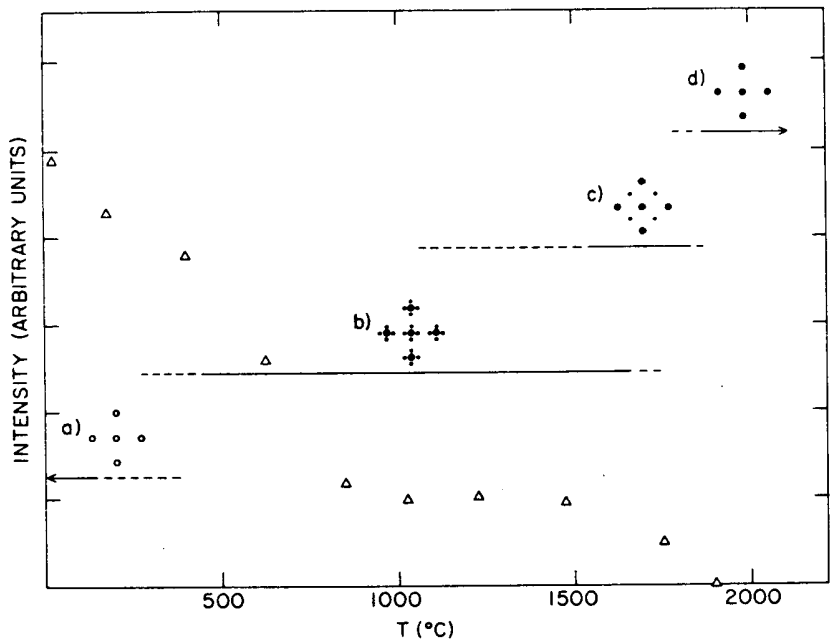

Fig. 1 - Intensity of the oxygen peak in Auger spectrum as a function of the sample thermal history. The different diffraction patterns observed at corresponding regions are indicated. (a) uncleaned Nb, covered with adsorbed oxygen; (b) faceted structure (Nb oxide); (c) monolayer (NbO) parallel to the substrate; (d) clean Nb surface. (from [4] and [13])

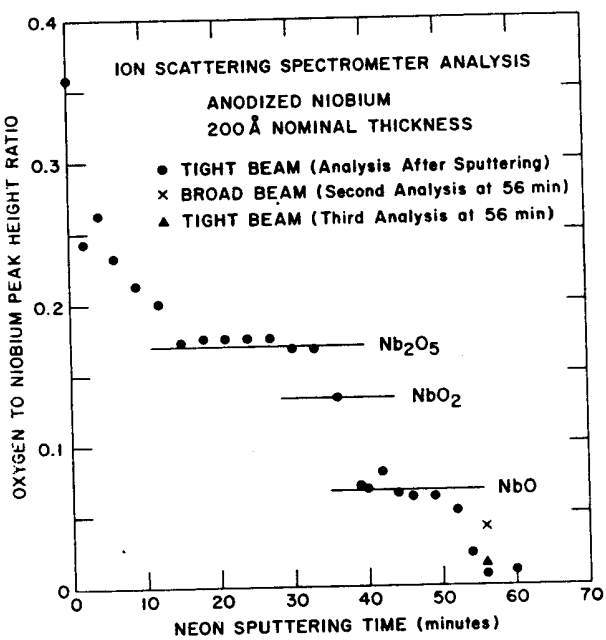

Fig. 2 - Ratio of heights of the O to Nb peaks in the ISS spectrum for a 200 Å anodized Nb surface plotted against sputtering time. (from [17]).

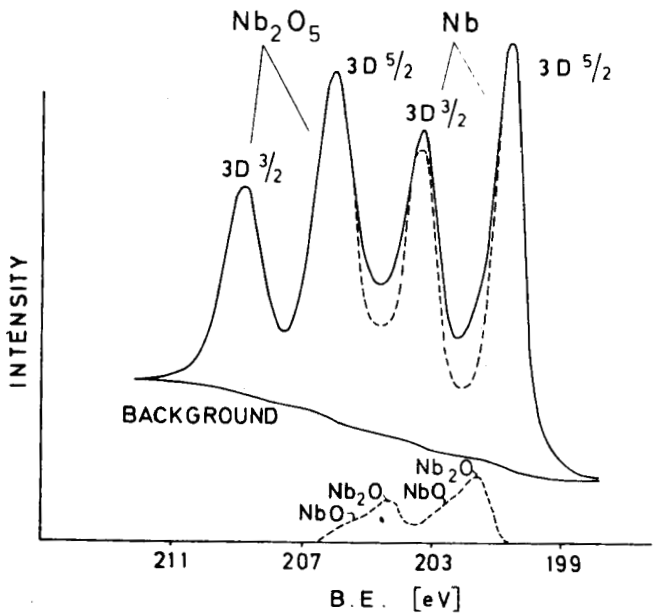

Fig. 3 - Typical XPS spectrum from a Nb surface around 200 eV. The double peaks correspond respectively to Nb and Nb^{5+}. After substracting the background, the dashed curves are obtained, which describe the lower oxides (from [19]).

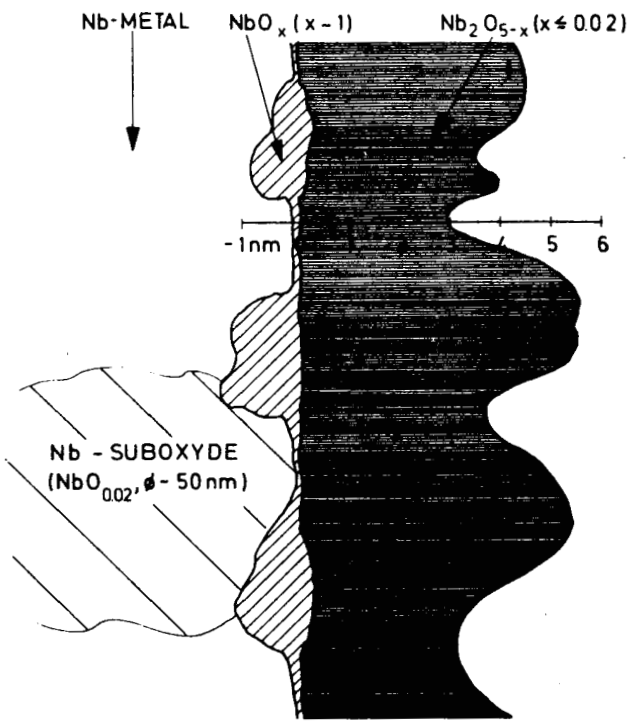

Fig. 4 - Results of an XPS study of Nb. Sketch of a wet oxidized Nb surface. (from [19]).

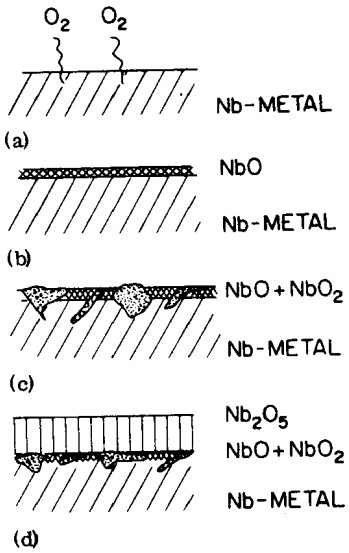

Fig. 5 - Results of an UPS study of Nb : schematic representation of the different stages for Nb (from [20]).

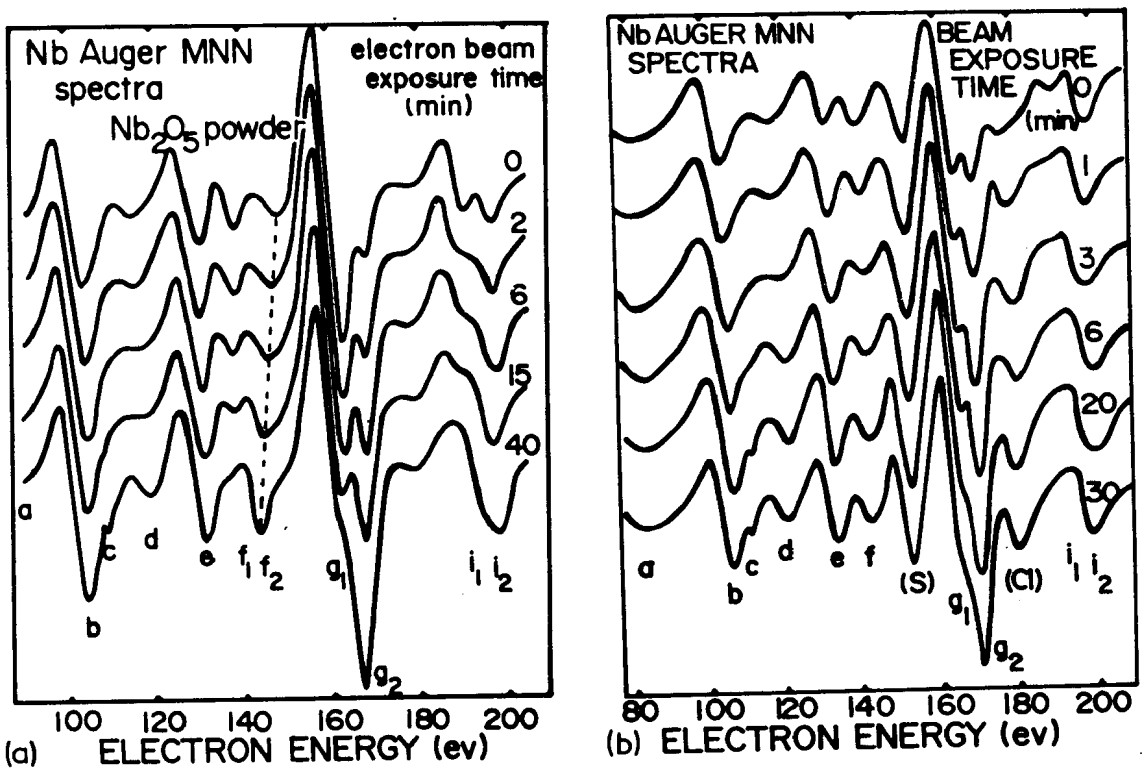

Fig. 6 - Variations of Auger spectra with beam exposure time.
(a) Nb_2O_5 powder ; beam voltage, 2 keV ; beam current, 15 μA.
(b) oxidized Nb foil. f_1, g_1, i_1 : "oxide" peaks (Nb^{5+}); f_2, g_2, i_2 : "metal" peaks (Nb).
The "metal" peak grows at the expense of its "oxide" counterpart (from [22]).

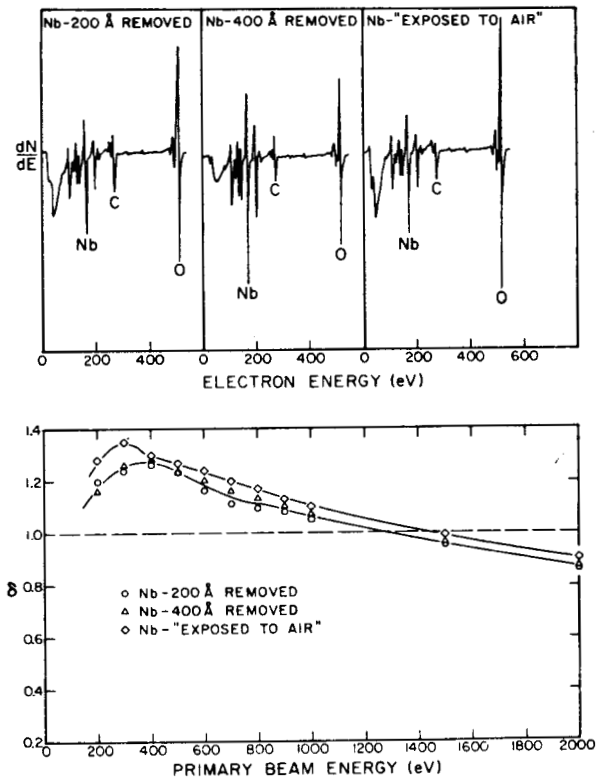

Fig. 7 - Secondary emission (SE) and Auger spectra for clean Nb and Nb exposed to air (from [27]).

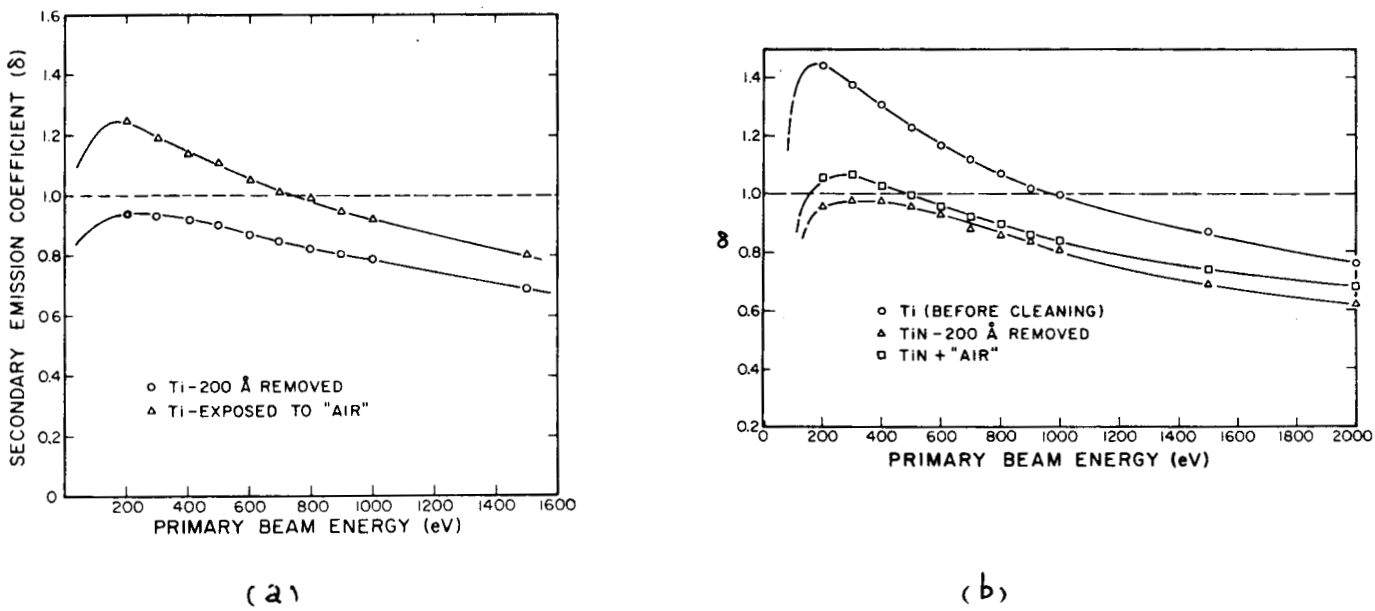

Fig. 8 - SE from Ti and TiN. (a) clean Ti and Ti exposed to air. (b) as-prepared, clean, and exposed to air TiN (from [27]).

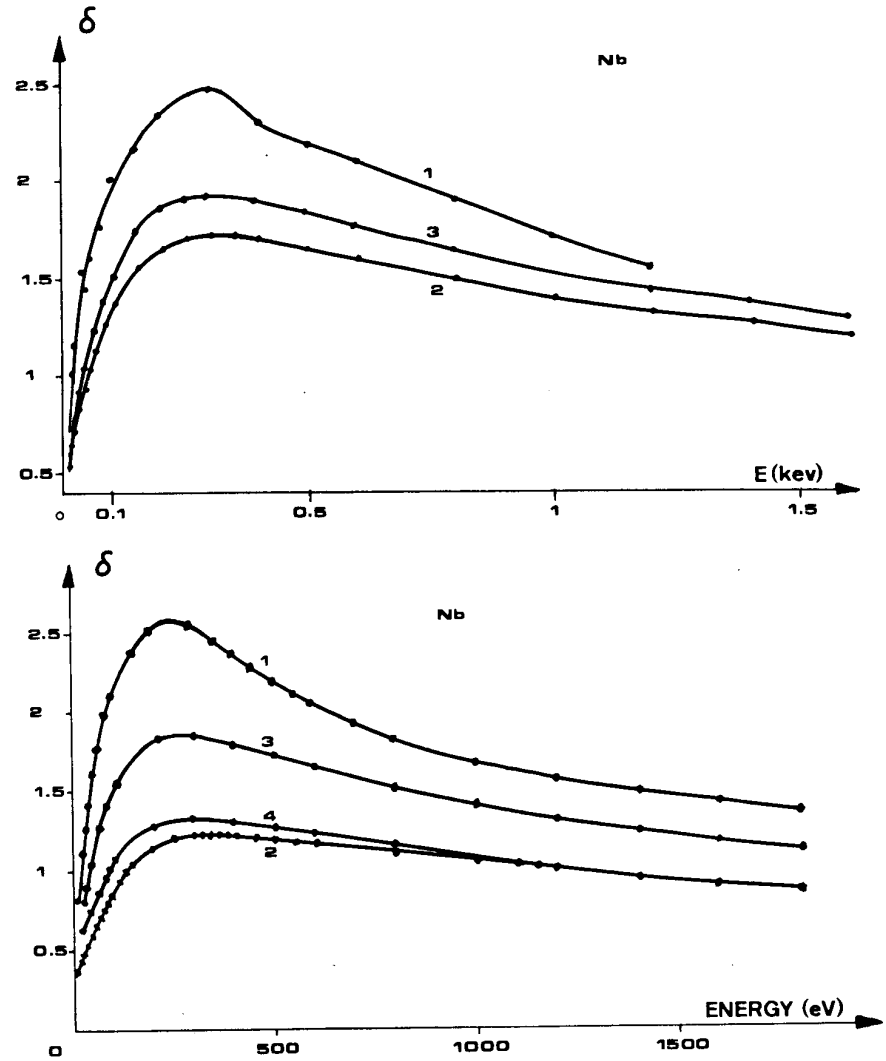

Fig. 9 - SE from Nb. (a) 1, unbaked; 2, baked; 3, baked + exposure to air. (b) 1, unbaked; 2, baked + gas discharge; 3, baked + g.d. + exp. to air; 4, 3 + g.d. (from [29]).

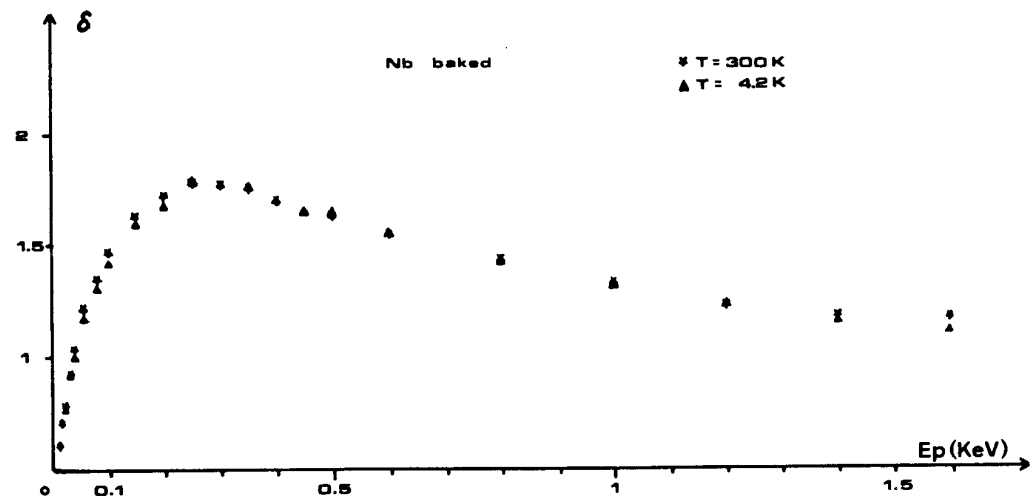

Fig. 10 - SE form a baked Nb surface. *, before cooling, Δ, after cooling to 4.2 K. (from [29]).

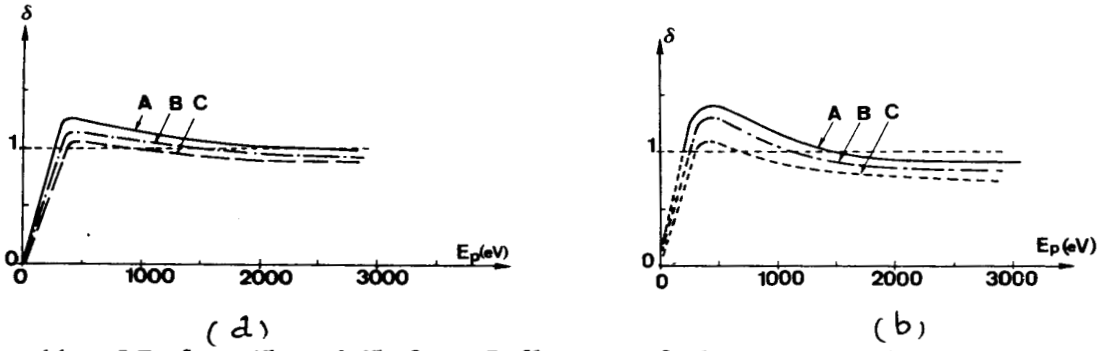

Fig. 11 - S E from Nb and Nb_2O_5 . Influence of the electron bombardment (E_p = 1000 eV; j_p = 10 μA/mm^2). A, t = 0; B, t = 5 min; C, t = 15 min. (a) Nb ; (b) Nb + 400 Å Nb_2O_5 (from [23])

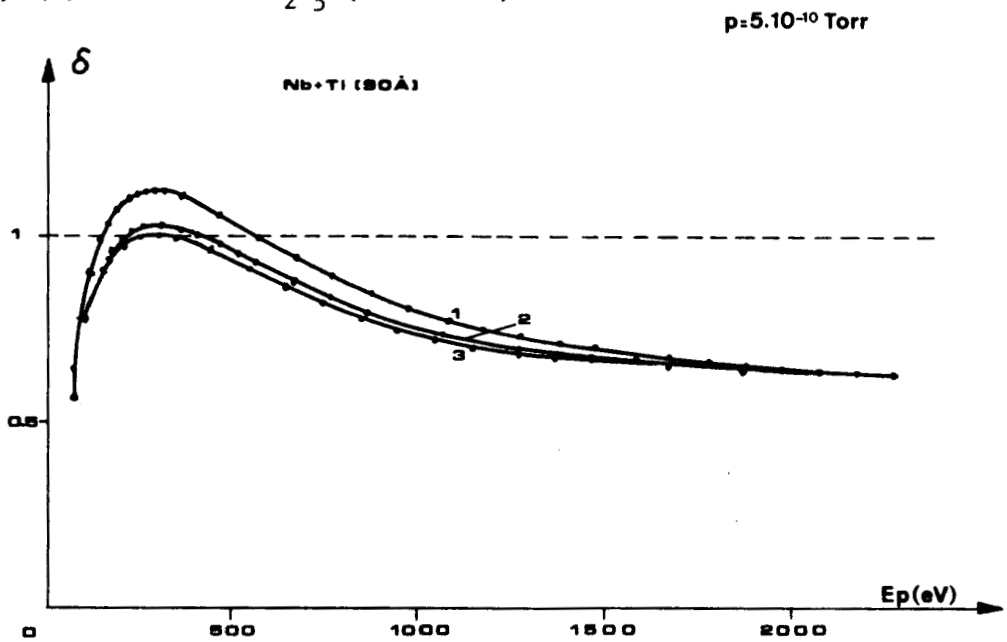

Fig. 12 - Influence of the electron bombardment on S E from thin Ti film on Nb, after baking. 1, t = 0; 2, t = 1 hour; 3, t = 15 hours (from [31])

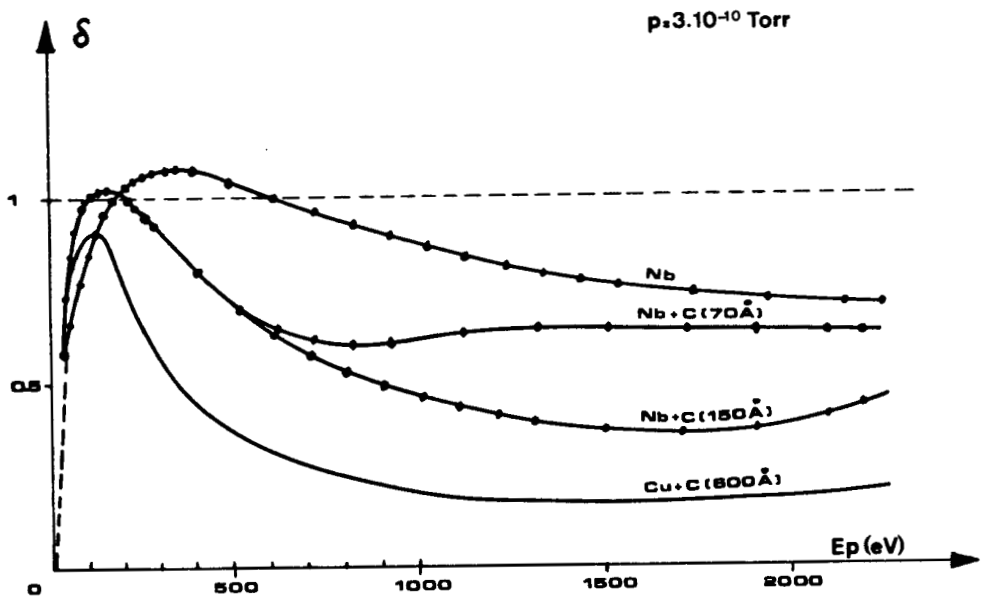

Fig. 13 - S E from thin C films, after baking and bombardment during about 1 hour. (from [31]).

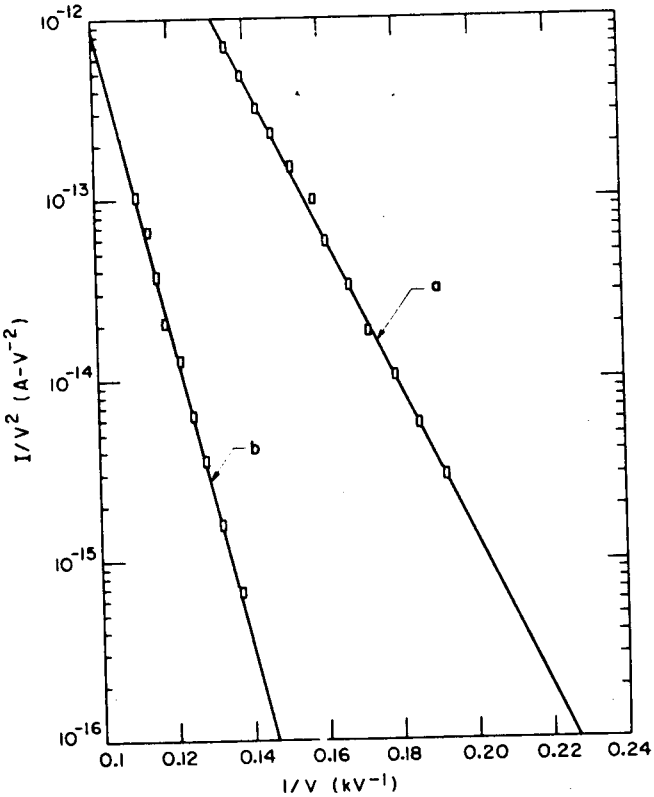

Fig. 14 - Fowler-Nordheim plots of d.c. field emission data.
(a) adsorbed atoms present on the emitting point surface.
(b) emission after cleaning of the tip by reverse field desorption. (from [33])

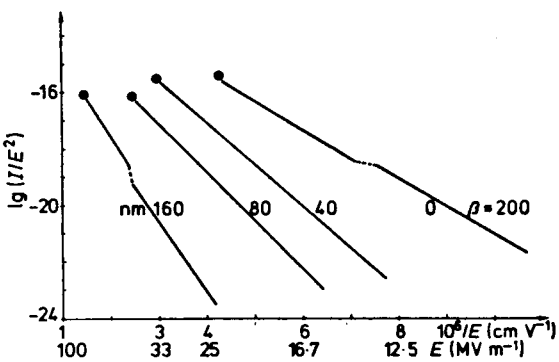

Fig. 15 - F.N. plots of current emitted by plane Nb electrodes covered with various oxide layer thickness (from [35]).

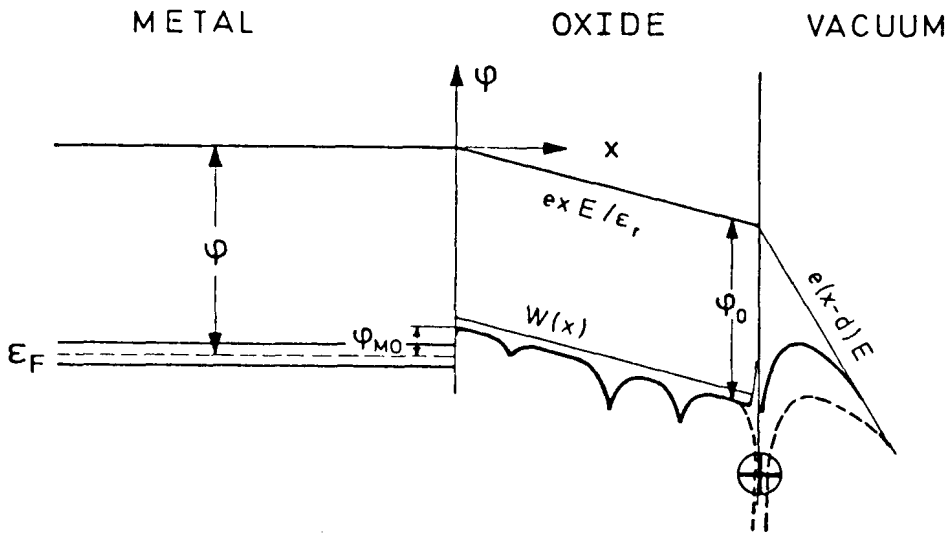

Fig. 16 - Electrochemical potential φ for electrons in an oxide coated ($\varepsilon_r > 1$) metal subject to the electric field E. The total emission current depends on the field emission into the oxide, the field assisted - hopping conduction through the oxide, and the field emission into vacuum, where the electrons tunnel through the indicated potential barriers (from [34]).